Soria-Verdugo, A., Rubio-Rubio, M., Goos, E. & Riedel, U. (2018). Combining the lumped capacitance method and the simplified distributed activation energy model to describe the pyrolysis of thermally small biomass particles. *Energy Conversion and Management*, vol. 175, pp. 164–172.

DOI: 10.1016/j.enconman.2018.08.097

Combining the Lumped Capacitance Method and the simplified Distributed Activation Energy Model to describe the pyrolysis of thermally small biomass particles

Antonio Soria-Verdugo[a]*, Mariano Rubio-Rubio[b], Elke Goos[c], Uwe Riedel[c]

[a] *Carlos III University of Madrid (Spain), Energy Systems Engineering Group, Thermal and Fluids Engineering Department. Avda. de la Universidad 30, 28911 Leganés (Madrid, Spain).*

[b] *University of Jaén (Spain), Division of Fluid Mechanics, Department of Mechanical and Mining Engineering. Campus de las Lagunillas, 23071 Jaén (Spain).*

[c] *Deutsches Zentrum für Luft- und Raumfahrt e.V. (German Aerospace Center, DLR), Institute of Combustion Technology, Pfaffenwaldring 38-40, 70569 Stuttgart (Germany).*

** corresponding author: asoria@ing.uc3m.es Tel: +34916248465.*

Abstract

The pyrolysis process of thermally small biomass particles was modeled combining the Lumped Capacitance Method (LCM) to describe the transient heat transfer and the Distributed Activation Energy Model (DAEM) to account for the chemical kinetics. The inverse exponential temperature increase predicted by the LCM was considered in the mathematical derivation of the DAEM, resulting in an Arrhenius equation valid to describe the evolution of the pyrolysis process under inverse exponential temperature profiles. The Arrhenius equation on which the simple LCM-DAEM model proposed is based was derived for a wide range of pyrolysis reactor temperatures, considering the chemical kinetics data of four

lignocellulosic biomass species: pine wood, olive kernel, thistle flower, and corncob. The LCM-DAEM model proposed was validated by comparison to the experimental results of the pyrolysis conversion evolution of biomass samples subjected to various inverse exponential temperature increases in a TGA. To extend the validation, additional biomass samples of Chlorella Vulgaris and sewage sludge were selected due to the different composition of microalgae and sludge compared to lignocellulosic biomass. The deviations obtained between the experimental measurements in TGA and the LCM-DAEM predictions for the evolution of the pyrolysis conversion, regarding the root mean square error of temperature, are below 5 ºC in all cases. Therefore, the simple LCM-DAEM model proposed can describe accurately the pyrolysis process of a thermally small biomass particle, accounting for both the transient heat transfer and the chemical kinetics by solving a simple Arrhenius equation.

Keywords**:** Biomass pyrolysis; Chlorella Vulgaris; Distributed Activation Energy Model (DAEM); Inverse exponential temperature increase; Lumped Capacitance Method (LCM); Sewage sludge.

Nomenclature

A	Pre-exponential factor [s^{-1}].
A_s	Surface of the solid particle [m^2].
α	Pyrolysis conversion [%].
Bi	Biot number [-].
β	Heating rate [ºC min^{-1}].
c	Heating parameter [min^{-1}].
c_s	Specific heat of the solid particle [J kg^{-1} K^{-1}].

d Particle diameter [mm].

E Activation energy [kJ mol^{-1}].

E_0 Mean value of gaussian distribution of activation energy [kJ mol^{-1}].

E_a Value of activation energy for which the step function changes [kJ mol^{-1}].

ϕ_{ie} Value of the ϕ-function for which the step function changes [-].

h Convection coefficient [W m^{-2} K^{-1}].

k Rate coefficient of a first-order reaction [s^{-1}].

k_s Thermal conductivity of the solid particle [W m^{-1} K^{-1}].

L_c Characteristic length [m].

ρ_s Density of the solid particle [kg m^{-3}].

R Universal gas constant [J mol^{-1} K^{-1}].

σ Standard deviation of gaussian distribution of activation energy [kJ mol^{-1}].

t Time [min].

T Temperature [ºC].

T_0 Ambient temperature [ºC].

T_∞ Reactor temperature [ºC].

V_s Volume of the solid particle [m^3].

Abbreviations:

CV Chlorella Vulgaris.

CFD Computational Fluid Dynamics.

DAEM Distributed Activation Energy Model.

HHV High Heating Value.

LCM Lumped Capacitance Method.

RMSE Root Mean Square Error.

SS Sewage Sludge.

74 TG Thermogravimetric.

75 TGA Thermogravimetric Analysis.

76 **1. Introduction**

77 Biomass is considered a promising substitute for fossil fuels due to its renewable
78 character, worldwide availability, and globally neutral net CO_2 emissions, based
79 on the carbon cycle. Biomass can be converted principally via biological or
80 thermochemical processes (McKendry 2002). The biological conversion uses
81 bacteria or enzymes to break the complex molecules of biomass into smaller
82 molecules. However, this process is much slower than thermochemical
83 conversion (Anca-Couce 2016). Thermochemical processing of biomass includes
84 pyrolysis, combustion, gasification, hydrothermal liquefaction, and hydrothermal
85 carbonization (Basu 2010). Among them, biomass pyrolysis, consisting in the
86 thermal degradation of the solid fuel at a temperature ranging from 300 to 600 ºC
87 in the absence of oxygen, has some beneficial characteristics. Biomass pyrolysis
88 is characterized by a low level of pollutant emissions derived from the conversion
89 process, obtaining a liquid bio-oil as the primary product, which can be readily
90 stored and transported, allowing its decentralized usage as a renewable fuel
91 (Czernik and Bridgwater, 2004).

92 The design and optimization of biomass pyrolysis reactors are currently based on
93 either Computational Fluid Dynamics (CFD) simulations or phenomenological
94 models (Sharma et al., 2015), which require in both cases a detailed knowledge
95 of the chemical kinetics of the thermal degradation reaction. In this sense, several
96 mathematical kinetic models are available in the literature, which can be classified
97 into kinetic-fitting and kinetic-free models (Bach and Chen, 2017). The former

involve the assumption for a functional form of the kinetic parameters, i.e., the activation energy and the pre-exponential factor. These fitting models include the single step model (Coats and Redfern, 1964), the sectional approach model (Lin et al., 2013), and the three pseudo-components model (Li et al., 2008). In contrast, kinetic-free models are based on experimental TGA measurements to calculate the activation energy and pre-exponential factor of the solid fuel pyrolysis reaction. The kinetic-free models comprise isoconversional models (Vyazovkin and Lesnicovich, 1992) and the simplified Distributed Activation Energy Model (DAEM) (Miura and Maki, 1998).

DAEM was developed initially by Vand (1943). The model was further simplified later by Miura (1995) and Miura and Maki (1998), resulting in a kinetic-free model known as simplified DAEM. Since then, this simplified DAEM has been widely used in the specific literature to describe the pyrolysis kinetics of a broad variety of solid fuels, including coal (Günes and Günes, 2008), charcoal (Várghegyi et al., 2002), polymers (Wanjun et al., 2005), lignocellulosic biomass (Sonobe and Worasuwannarak, 2008), microalgae (Ceylan and Kazan, 2015), sewage sludge (Soria-Verdugo et al., 2013), oil shale (Wang et al., 2009), and medical waste (Yan et al., 2009). The simplified DAEM has been proven to derive accurate results for the kinetic parameters of biomass pyrolysis from TGA measurements. However, its applicability estimating the evolution of the pyrolysis conversion with temperature is limited by the fact that simplified DAEM is valid exclusively for constant heating rates of the solid particles, i.e., linear increases of temperature with time. Nevertheless, the temperature increase of solid particles in pyrolysis reactors is typically non-linear and, therefore, the direct application of the simplified DAEM in these reactors is not possible.

123 This paper deals with the limitation of the simplified DAEM to constant heating
124 rates and is devoted to overcoming this limit. A simple model is proposed to
125 describe the pyrolysis of thermally small particles, combining the Lumped
126 Capacitance Method (LCM), to estimate the transient heat transfer of the solid
127 particles, and the simplified Distributed Activation Energy Model (DAEM), to
128 account for the chemical kinetics of the thermal degradation. The proposed LCM-
129 DAEM model is based on an Arrhenius equation obtained following the
130 mathematical procedure proposed by Miura (1995) and Miura and Maki (1998)
131 for the simplified DAEM, but considering the inverse exponential temperature
132 increase to which thermally small particles are subjected according to the LCM.
133 The new Arrhenius equation for the LCM-DAEM was derived as a function of the
134 reactor temperature, considering the pyrolysis kinetic data of several
135 lignocellulosic biomass species. Finally, the validity of the Arrhenius equations
136 derived was validated comparing the estimation of the pyrolysis conversion
137 evolution predicted by the proposed LCM-DAEM model to experimental pyrolysis
138 measurements of microalgae and sewage sludge, conducted in a
139 thermogravimetric analyzer (TGA) under various inverse exponential
140 temperature increases.

141 **2. Theoretical Model**

142 Pyrolysis of solid fuels is a complex process which involves both heat transfer
143 and chemical reactions. In this regard, a simplified model is proposed to describe
144 the pyrolysis reactions of small biomass particles. The model proposed is based
145 on combining the Lumped Capacitance Method to consider heat transfer between

146 the environment and the solid particle with the simplified Distributed Activation
147 Energy Model to account for the chemical kinetics of the pyrolysis reactions.

148 **2.1. Lumped Capacitance Method (LCM)**

149 When a biomass particle is fed to a reactor at a high temperature T_∞, transient
150 conduction occurs inside the particle, whose temperature increases with time. If
151 the temperature inside the particle can be considered spatially uniform, a single
152 temperature T can be employed to describe the time evolution of heat transfer
153 between the reactor and the particle. This assumption is the base of the widely
154 known Lumped Capacitance Method, for which the temperature of the particle
155 can be determined by formulating a global energy balance on the particle, relating
156 the convection heat transfer rate at the particle surface with the rate of change of
157 internal energy of the particle:

158 $$h \cdot A_s \cdot \left(T_\infty - T\right) = \rho_s \cdot V_s \cdot c_s \frac{\mathrm{d}T}{\mathrm{d}t}, \quad (1)$$

159 where h is the convection coefficient, T_∞ is the reactor temperature, T is the
160 temperature inside the particle, t is time, and A_s, V_s, ρ_s, and c_s are the solid particle
161 surface, volume, density, and specific heat, respectively.

162 Integrating Eq. (1), considering the initial temperature of the solid particle T_0 when
163 the particle is fed to the reactor, i.e., at the initial time t = 0, the time evolution of
164 the particle temperature is obtained as an inverse exponential approximation to
165 the reactor temperature T_∞:

166 $$T = T_\infty - \left(T_\infty - T_0\right) \cdot \exp\left(-\frac{h \cdot A_s}{\rho_s \cdot V_s \cdot c_s} t\right). \quad (2)$$

167 The time-coefficient in the exponential function in Eq. (2) can be defined as the
168 heating parameter:

169 $$c = \frac{h \cdot A_s}{\rho_s \cdot V_s \cdot c_s}, \quad (3)$$

170 which is constant for a specific biomass type, i.e., fixed values of A_s, V_s, ρ_s, and
171 c_s, and reactor operating conditions, i.e., uniform value for h.

172 The essence of the LCM is the assumption of uniform spatial temperature
173 distribution inside the solid particle during the transient heating process.
174 Therefore, the validity of the LCM and, thus, of Eq. (2) to describe the temperature
175 evolution of biomass particles, should be discussed in the light of that hypothesis.
176 In that sense, the Biot number Bi is defined for transient conduction problems as
177 the ratio of the thermal resistance by conduction inside the solid particle and the
178 thermal resistance by convection at the particle surface, obtaining:

179 $$Bi = \frac{h \cdot L_c}{k_s}, \quad (4)$$

180 where h is the convection coefficient, k_s is the thermal conductivity of the solid
181 particle, and L_c is the characteristic length, defined as the ratio between the solid
182 particle volume V_s and its surface A_s.

183 Therefore, if $Bi \ll 1$, the thermal resistance by conduction inside the solid particle
184 is negligible compared to the thermal resistance by convection at its surface.
185 Thus, the assumption of spatially uniform temperature is reasonable for cases
186 with $Bi \ll 1$. In practice, the validity criterion for the central assumption of the
187 LCM is $Bi \leq 0.1$, and a low error associated to the LCM can be expected when

188 this validity criterion is satisfied (Incropera et al., 2007). The particles for which
189 this criterion is met are called thermally small particles.

190 Assuming a spherical shape for the solid particles, the characteristic length can
191 be related to the particle diameter d as $L_c = d/6$. In the case of biomass particles
192 heated up in a reactor, typical values for the convection coefficient are $h \sim 20$
193 W/m^{2}K, and thermal conductivity is approximately $k_s \sim 0.1$ W/m·K, and therefore
194 the validity criterion for the LCM is satisfied provided that the particle diameter is
195 $d \leq 3$ mm. In conclusion, the LCM can be used to estimate the particle
196 temperature increase for small size biomass particles, such as short straws or
197 olive stones, which are typically obtained fragmented as a residue of the olive oil
198 industry (Pattara et al., 2010). In contrast, for those cases in which $Bi > 0.1$,
199 appreciable temperature differences within these bigger solid particles exist.
200 Then, spatial effects should be considered, and the heat equation must be solved
201 to determine the temperature distribution inside these bigger particles.

202 **2.2. Distributed Activation Energy Model (DAEM)**

203 The simplified Distributed Activation Energy Model is widely used to describe the
204 chemical kinetics of solid fuels pyrolysis. DAEM considers the solid fuel as a
205 complex mixture of components, which decompose as a result of a large number
206 of independent irreversible first-order reactions, with different associated
207 activation energies, occurring either simultaneously or consecutively. The
208 conversion α during the pyrolysis reaction can be determined as follows:

209 $$1-\alpha = \int_0^{\infty} \exp\left(-A\int_0^t \mathrm{e}^{E/RT}\,\mathrm{d}t\right) f\left(E\right)\cdot \mathrm{d}E, \qquad (5)$$

where α is the pyrolysis conversion at time *t*, *A* is the pre-exponential factor, *E* is the activation energy, *R* is the universal gas constant, *T* is the temperature, and *f(E)* is the probability density function of the activation energy. The exponential term in Eq. (5) is the so-called ϕ function:

$$\phi = \exp\left(-A\int_0^t \mathrm{e}^{-E/RT}\,\mathrm{d}t\right). \tag{6}$$

Considering a constant heating rate β, i.e., a linear temperature increase $T = \beta \cdot t$, the time integral in the ϕ function is converted to a temperature integral, which can be simplified using the approximation of Coats and Redfern (1964) as follows:

$$\phi = \exp\left(-\frac{A}{\beta}\int_0^T \mathrm{e}^{-E/RT}\,\mathrm{d}T\right) \approx \exp\left(-\frac{ART^2}{\beta E}\mathrm{e}^{-E/RT}\right). \tag{7}$$

This expression for the ϕ function can be approximated as a step function at a value of the activation energy of $E = E_a$, obtaining the following expression for the pyrolysis conversion α, taking into account the normalization criterion for the probability density function of activation energies *f(E)*:

$$\alpha = 1 - \int_{E_a}^{\infty} f\left(E\right)\cdot \mathrm{d}E = \int_0^{E_a} f\left(E\right)\cdot \mathrm{d}E. \tag{8}$$

The value of the ϕ function for which the step function changes, i.e., the value of ϕ for $E = E_a$, should be established. Miura (1995) proposed a value of $\phi(E_a) = 0.58$, which was found to be valid for a broad variety of biomass samples. Therefore, using this value for the ϕ function, and taking the logarithm to Eq. (7), the Arrhenius equation for the simplified DAEM is obtained:

$$\ln\left(\frac{\beta}{T^2}\right) = \ln\left(\frac{AR}{E}\right) + 0.6075 - \frac{E}{R}\frac{1}{T}. \tag{9}$$

Considering this Arrhenius equation, Miura and Maki (1998) proposed a procedure to determine the activation energy *E* and the pre-exponential factor *A* of the pyrolysis reaction based on thermogravimetric pyrolysis measurements conducted for various heating rates β.

However, the main limitation of this widely used simplified DAEM is its restriction to constant heating rates, i.e., linear increases of temperature with time. To avoid this limitation, the mathematical procedure of simplified DAEM was modified by Soria-Verdugo et al. (2016) to derive Arrhenius equations for parabolic and positive exponential temperature increases. Nevertheless, no Arrhenius equation available in the literature can describe the pyrolysis kinetics under inverse exponential temperature increases, such as those predicted by the LCM, Eq. (2). In this regard, the following subsection presents the mathematical derivation of an Arrhenius equation, based on the simplified DAEM, valid for inverse exponential temperature increases of the solid particles, as modeled by the LCM.

2.3. Combined LCM and simplified DAEM (LCM-DAEM)

The pyrolysis of thermally small particles, i.e., *Bi* < 0.1, can be modeled by combining the LCM to characterize the transient heat transfer and the simplified DAEM to describe the chemical kinetics. Deriving the inverse exponential temperature increase predicted by the LCM, Eq. (2), the time variation can be related to the temperature variation as follows:

$$\mathrm{d}t = \frac{\mathrm{d}T}{c\left(T_\infty - T\right)}. \tag{10}$$

Therefore, the time integral in the ϕ function, Eq. (6), can be converted to a temperature integral, considering an inverse exponential temperature increase, using Eq. (10):

$$\phi = \exp\left(-\frac{A}{c} \int_0^T \frac{\mathrm{e}^{-E/RT}}{T_\infty - T} \mathrm{d}T \right). \tag{11}$$

The temperature integral in Eq. (11) can be rewritten, using a substitution method, in terms of a new pair of variables, $z = E/(RT)$ and $z_\infty = E/(RT_\infty)$:

$$\int_0^T \frac{\mathrm{e}^{-E/RT}}{T_\infty - T} \mathrm{d}T = \int_z^\infty \frac{\mathrm{z}_\infty \mathrm{e}^{-z}}{z\left(z - \mathrm{z}_\infty\right)} \mathrm{d}z. \tag{12}$$

The solution to this integral is:

$$\int_z^\infty \frac{\mathrm{z}_\infty \mathrm{e}^{-z}}{z\left(z - \mathrm{z}_\infty\right)} \mathrm{d}z = \mathrm{e}^{-\mathrm{z}_\infty} \mathrm{Ei}\left(z - \mathrm{z}_\infty\right) - \mathrm{Ei}\left(z\right), \tag{13}$$

where Ei(z) is the exponential integral, which can be approximated to (Bleistein and Handelsman, 1987):

$$\mathrm{Ei}\left(z\right) = \frac{\mathrm{e}^{-z}}{z} \sum_{n=0}^{\infty} \frac{n!}{\left(-z\right)^n}, \tag{14}$$

and therefore:

$$\mathrm{Ei}\left(z - z_\infty\right) = \frac{\mathrm{e}^{-\left(z - z_\infty\right)}}{z - z_\infty} \sum_{n=0}^{\infty} \frac{n!}{\left(-z + z_\infty\right)^n}, \tag{15}$$

Thus, considering these approximations for the exponential integrals, Eq. (13) can be expressed as follows:

$$\int_z^{\infty} \frac{z_{\infty} e^{-z}}{z\left(z - z_{\infty}\right)} dz = e^{-z} \sum_{n=1}^{\infty} (-1)^{n-1} (n-1)! \left[\left(z - z_{\infty}\right)^{-n} - z^{-n} \right], \quad (16)$$

which, in terms of the original variables, provides an approximation to the temperature integral in Eq. (11) that reads:

$$\int_0^T \frac{e^{-E/RT}}{T_{\infty} - T} dT = e^{-E/RT} \sum_{n=1}^{\infty} (-1)^{n-1} (n-1)! \left(\frac{R}{E}\right)^n \left[\left(\frac{T \cdot T_{\infty}}{T_{\infty} - T}\right)^n - T^n \right]. \quad (17)$$

Considering typical values of the activation energy of biomass pyrolysis of $E \sim$ 200 kJ/mol, biomass pyrolysis temperature of $T \sim 300$ ºC, and the universal gas constant $R = 8.314$ J/mol, a low error would be committed by approximating the temperature integral to the first term (n = 1) in Eq. (17), provided that the reactor temperature is around 250 ºC above the characteristic temperature of biomass pyrolysis, i.e., $T_{\infty} - T > 250$ ºC. Considering this approximation for the temperature integral, the ϕ function, Eq. (11), yields:

$$\phi \approx \exp\left(-\frac{ART^2}{cE\left(T_{\infty} - T\right)} \right). \quad (18)$$

Following the same mathematical procedure as for the original simplified DAEM, valid only for linear temperature increases, the exponential expression of the ϕ function obtained for inverse exponential temperature increases, Eq. (18), is approximated to a step function changing at an activation energy $E = E_a$. Then, according to Eq. (5), the pyrolysis conversion α can be written as follows:

$$\alpha = 1 - \int_0^{\infty} \phi \cdot f(E) \cdot dE = 1 - \int_{E_a}^{\infty} f(E) \cdot dE = \int_0^{E_a} f(E) \cdot dE. \quad (19)$$

Thus, the value of the activation energy for which the step function changes, $E = E_a$, can be determined satisfying the second equality in Eq. (19), that is:

$$\int_0^{\infty} \phi \cdot f(E) \cdot \mathrm{d}E = \int_{E_a}^{\infty} f(E) \cdot \mathrm{d}E, \tag{20}$$

and, once this activation energy E_a is obtained, the value of the ϕ function $\phi(E_a) = \phi_{ie}$ is determined substituting in Eq. (11). To determine the activation energy E_a from Eq. (20), a statistical distribution needs to be assumed for $f(E)$, with the Gaussian distribution being the most typical assumption (Cai and Liu, 2008; Cai et al., 2014):

$$f(E) = \frac{1}{\sigma\sqrt{2\pi}} \exp\left(-\frac{(E - E_0)^2}{2\sigma^2} \right), \tag{21}$$

where E_0 is the mean and σ the standard deviation of the activation energy probability distribution.

The procedure to determine E_a from the fulfilment of Eq. (20) was followed by Miura (1995), using various biomass samples, to determine the proper value of the ϕ function for linear temperature increases, obtaining a value of $\phi(E_a) = 0.58$. This procedure was also followed in a previous work by Soria-Verdugo et al. (2016) to determine the values of $\phi(E_a)$ for both parabolic and positive exponential temperature increases. In this previous work, the pyrolysis chemical kinetic data of four lignocellulosic biomasses were employed to calculate the proper values of $\phi(E_a)$, obtaining reliable values. Therefore, the calculation of the ϕ function value for inverse exponential temperature increases $\phi(E_a) = \phi_{ie}$ will also be based on the same kinetic data of pine wood, olive kernel, thistle flower, and corncob

306 as in Soria-Verdugo et al. (2016). This kinetic data, included in Table 1, were
307 obtained for the distributions of activation energy and pre-exponential factor as a
308 function of the pyrolysis conversion reported in Soria-Verdugo et al. (2015).

309 Table 1. Pyrolysis kinetic data of various lignocellulosic biomass species.
310

Sample	E_0 [kJ/mol]	σ [kJ/mol]	A [s^{-1}]
Pine wood	165.0	2.6	$1.57 \cdot 10^{12}$
Olive kernel	162.2	3.2	$4.11 \cdot 10^{12}$
Thistle flower	154.5	1.6	$2.80 \cdot 10^{11}$
Corncob	183.5	5.0	$2.31 \cdot 10^{14}$

311

312 Using the mean E_0 and standard deviation σ of the activation energy, the
313 probability distribution $f(E)$ can be built using Eq. (21), and the value of the
314 activation energy E_a for which the ϕ function changes can be obtained from
315 satisfying Eq. (20). Once the value of E_a is obtained, the value of $\phi(E_a) = \phi_{ie}$ can
316 be calculated from Eq. (18). However, for inverse exponential temperature
317 increases as those predicted by the LCM, since the ϕ function obtained, Eq. (18),
318 depends on the reactor temperature T_∞, the value of $\phi(E_a) = \phi_{ie}$ is also expected
319 to be a function of this reactor temperature. Therefore, the process proposed by
320 Miura (1995) to determine $\phi(E_a)$ will be followed for various reactor temperatures,
321 to determine the dependence of ϕ_{ie} on T_∞.

322 As an example, the process to determine ϕ_{ie} is shown graphically in Figure 1 for
323 pine wood at T_∞ = 550 ºC and T_∞ = 650 ºC. First, using the kinetic data included
324 in Table 1, the probability density function of the activation energy $f(E)$ is built
325 employing Eq. (21). Secondly, the approximation of the ϕ function, Eq. (18), is
326 used to determine the curve $\phi \cdot f(E)$. Then, the value of E_a is determined as the

activation energy for which Eq. (20) is satisfied, i.e., the area under the curve of *f(E)* from this activation energy E_a to infinity equals the whole area under the curve $\phi \cdot f(E)$. Finally, using the simplification of the ϕ function, Eq. (18), the value of the ϕ function for this activation energy is obtained $\phi(E_a) = \phi_{ie}$. Figure 1 shows that, as expected, the value of ϕ_{ie} is a function of T_∞, due to the dependence of the ϕ function on the reactor temperature. For a reactor temperature of T_∞ = 550 ºC, the value obtained for the ϕ function is ϕ_{ie} = 0.482, whereas for a temperature of T_∞ = 650 ºC this value is ϕ_{ie} = 0.550. Similar results to those shown in Figure 1 for pine wood were obtained for the other three lignocellulosic biomass species considered (olive kernel, thistle flower, and corncob) resulting in similar values of ϕ_{ie}, thus, these results are not shown graphically to avoid repetition. In the plots of the ϕ function included in Figure 1, a sharp variation of ϕ can be observed in the typical range of activation energies for biomass pyrolysis, from 100 to 250 kJ/mol, which justifies the simplification of considering the ϕ function as a step function.

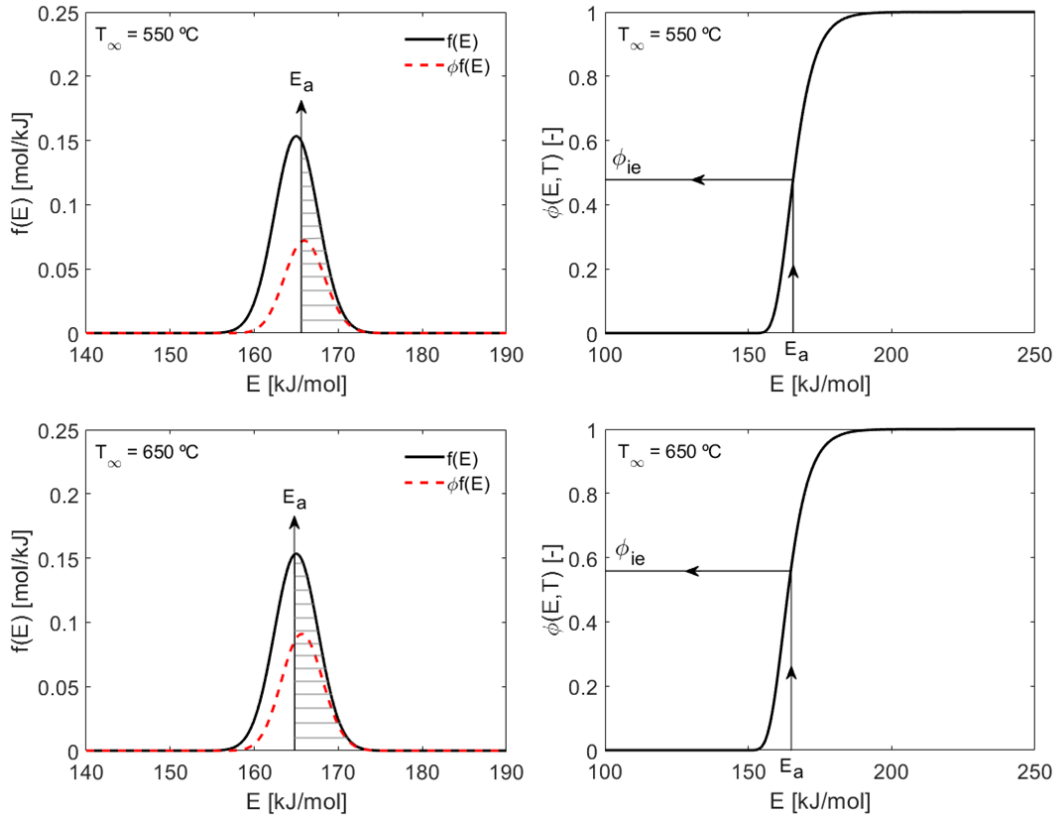

342

343 Figure 1. Process to determine ϕ_{ie}.

344 To determine the dependence of ϕ_{ie} on T_∞, the procedure described in Figure 1
345 was repeated for each lignocellulosic sample included in Table 1, varying the
346 reactor temperature T_∞ from 450 to 750 ºC in intervals of 10 ºC. Similar values of
347 ϕ_{ie} were obtained for the different samples for each reactor temperature.
348 Therefore, the values of ϕ_{ie} determined for each biomass specie were averaged
349 to obtain the dependence of ϕ_{ie} on T_∞. The averaged values of ϕ_{ie} are depicted in
350 Figure 2 as a function of the reactor temperature T_∞, together with a parabolic
351 fitting of the values obtained. The parabolic fitting of ϕ_{ie} with T_∞, shown in Figure
352 2, follows the equation:

353 $$\phi_{ie} = -1.533 \cdot 10^{-6} \cdot T_\infty^{\,2} + 2.577 \cdot 10^{-3} \cdot T_\infty - 0.4745, \quad (22)$$

354 with T_∞ in ºC. This parabolic relation describes accurately the dependence of ϕ_{ie}
355 on T_∞, obtaining a determination coefficient R^2 for the fitting higher than 0.99.

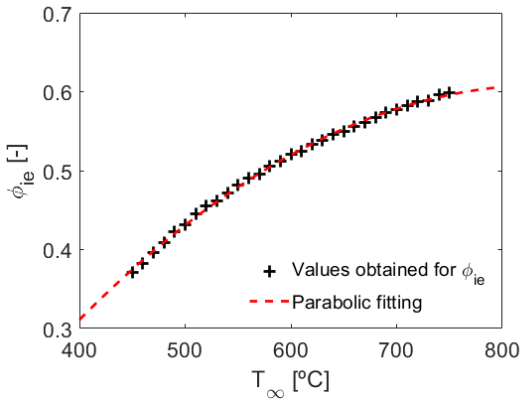

356

357 Figure 2. Values obtained for ϕ_{ie} as a function of the reactor temperature T_∞
358 (black +) and parabolic fitting (red dashed line).

359 The value of ϕ_{ie} can be used in the simplification of the ϕ function, Eq. (18), to
360 derive the Arrhenius equation for inverse exponential temperature increases. By
361 taking the logarithm twice and rearranging terms, the following expression is
362 obtained:

363 $$\ln\left(\frac{c\left(T_\infty - T\right)}{T^2}\right) = \ln\left(\frac{AR}{E}\right) - \ln\left(-\ln\left(\phi_{ie}\right)\right) - \frac{E}{R}\frac{1}{T} \tag{23}$$

364 Therefore, using Eq. (22) to calculate the value of ϕ_{ie} as a function of the reactor
365 temperature T_∞, an Arrhenius equation can be derived for a specific reactor
366 temperature. For instance, for thermally small biomass particles in reactors at
367 temperatures of 550 ºC and 650 ºC, the Arrhenius equations that describe the
368 pyrolysis process read:

369 $$\ln\left(\frac{c\left(T_\infty - T\right)}{T^2}\right) = \ln\left(\frac{AR}{E}\right) + 0.3070 - \frac{E}{R}\frac{1}{T}, \quad \text{for } T_\infty = 550\ ^\circ\text{C} \tag{24}$$

370 $$\ln\left(\frac{c\left(T_\infty - T\right)}{T^2}\right) = \ln\left(\frac{AR}{E}\right) + 0.5233 - \frac{E}{R}\frac{1}{T}, \quad \text{for } T_\infty = 650\ ^\circ\text{C} \tag{25}$$

371 These simple Arrhenius equations describe the whole pyrolysis process of
372 thermally small biomass particles when they are fed to a reactor at a higher
373 temperature T_∞. Thus, provided that the pyrolysis kinetic parameters, i.e., E and
374 A, of the biomass employed are known as a function of the pyrolysis conversion
375 α, and that the heating parameter c, Eq. (3), is estimated, the calculation of the
376 temperature for which each conversion occurs can be carried out by solving the
377 transcendental Arrhenius equation for specific values of the pyrolysis conversion.
378 Therefore, an estimation of the mass released during the pyrolysis of thermally
379 small biomass particles as a function of temperature or time, considering Eq. (2),
380 can be made by solving the Arrhenius equation corresponding to the reactor
381 temperature employed (see Eq. (24) or Eq. (25)). The calculations were done
382 with units of K and s for temperature and time, respectively, to be in agreement
383 with the international system of units. However, to increase the readability of the
384 paper, temperature values were reported in °C and time in min, and
385 consequently, the heating rates and heating parameters were reported in K/min
386 and min^{-1}, respectively.

387 Since the proposed LCM-DAEM model combines the LCM to describe the
388 transient heat transfer problem and simplified DAEM to account for the chemical
389 kinetics of the biomass pyrolysis process, it is subjected to the limitations of both
390 methods. Therefore, the maximum size of the particles for which the proposed
391 model is valid is limited, and must satisfy the condition of $\text{Bi} \leq 0.1$, and the
392 pyrolysis reactions are assumed to follow all first-order kinetics, which is a general
393 hypothesis of DAEM. In addition, the heating parameter c was considered to be

394 constant during the derivation of the LCM-DAEM model. However, the variables
395 affecting the heating parameter *c*, Eq. (3), might be subjected to changes during the
396 biomass pyrolysis, although the range of variation of these variables would be restricted
397 by the limited size of the particles imposed by the LCM. Thus, considering a constant
398 value of *c* for the derivation of the model is a reasonable assumption. Nevertheless, if
399 information about the variation of the heating parameter *c*, or its affecting parameters, is
400 available, the LCM-DAEM model could be modified to account also for variations of *c*.

401 **3. Materials and Methods**

402 **3.1. Thermogravimetric Analyzer**

403 The pyrolysis measurements were conducted in a thermogravimetric analyzer
404 TGA Q500 from TA Instruments. The inert atmosphere required for pyrolysis
405 conditions was guaranteed by supplying a flow rate of 60 ml/min of nitrogen 3.0
406 to the furnace. A small mass of the sample of 10.0±0.5 mg, composed of particles
407 under 100 μm, was employed for the tests to limit heat and mass transfer effects
408 inside the sample. Thus, using this small sample size, the temperature of the
409 sample is assumed to be that imposed by the TGA furnace, which in this case
410 will be inverse exponential temperature increases as those predicted by the LCM.
411 Considering the sensitivity of the TGA mass measurement of 0.1 μg and the
412 weighing precision of ±0.01%, the sample mass used provides a high signal-to-
413 noise ratio.

414 To check the validity of the proposed LCM-DAEM model using TGA pyrolysis
415 measurements, inverse exponential temperature increases as those predicted by
416 the LCM, Eq. (2), should be programmed to the TGA. However, the TGA permits
417 only constant heating rates, i.e., linear increases in temperature with time.

418 Therefore, the inverse exponential temperature profiles required were built from
419 a series of 25 constant heating rates, as described in Soria-Verdugo et al. (2016)
420 for parabolic and positive exponential temperature increases. Two different
421 inverse exponential temperature increases, corresponding to heating parameters
422 of c = 0.06 min^{-1} and c = 0.18 min^{-1}, were built to heat the samples in the TGA
423 furnace up to two different temperatures of T_∞ = 550 ºC and T_∞ = 650 ºC. The
424 heating parameters tested were selected to limit the values of the 25 constant
425 heating rates composing the inverse exponential temperature profiles to
426 operative values for the TGA employed. For the two heating parameters and
427 reactor temperatures selected, the constant heating rates required to build the
428 temperature profiles range between 0.03 ºC/min and 100 ºC/min, values that can
429 be handled in the TGA Q500 used. In fact, heating rates up to 200 ºC/min can be
430 programmed in this equipment (Soria-Verdugo et al., 2014). A blank experiment
431 was also conducted for each heating parameter and reactor temperature to
432 subtract buoyancy effects, and the repeatability of the pyrolysis tests was
433 checked by repeating each run three times, obtaining relative discrepancies lower
434 than 0.5%.

435 **3.2. Biomass Characterization**

436 The derivation of the Arrhenius equation for the LCM-DAEM model proposed was
437 based on the ϕ_{ie} values obtained from the pyrolysis kinetics data of four
438 lignocellulosic biomass species, typically composed of hemicellulose, cellulose,
439 lignin, and low amounts of inorganic matter. Therefore, the validation of the model
440 was performed by comparing TGA pyrolysis measurements of non-lignocellulosic
441 biomass samples to the predictions of the model, to prove the validity of the
442 proposed equations for a broad range of biomass types. In this regard, biomass

443 samples of microalgae, which are composed of carbohydrates, proteins, lipids,
444 and other minor components, and sewage sludge (SS), which comprises organic
445 and inorganic matter, were analyzed. Among the different microalgae species,
446 Chlorella Vulgaris (CV) was selected since it is widely grown and used (Figueira
447 et al., 2015).

448 The basic characterization of the microalgae and sewage sludge tested are
449 shown in Table 2. The characterization consists in a proximate analysis,
450 performed in the TGA Q500 from TA Instruments, an ultimate analysis, carried
451 out in a LECO TruSpec CHN Macro and TruSpec S analyzer, and a heating value
452 test, conducted in a Parr 6300 isoperibolic calorimeter. The results for the
453 Chlorella Vulgaris sample were reported in Soria-Verdugo et al. (2018), whereas
454 the sewage sludge results were taken from Soria-Verdugo et al. (2017a).
455 However, in the case of the sewage sludge, the sulfur content was measured in
456 the LECO TruSpec S analyzer to include the complete data in Table 2.

457 Table 2. Results of the basic characterization of Chlorella Vulgaris and sewage
458 sludge (PA: Proximate Analysis, UA: Ultimate Analysis, VM: Volatile Matter, A:
459 Ash, C: Carbon, H: Hydrogen, N: Nitrogen, S: Sulfur, O: Oxygen, HHV: High
460 Heating Value, db: dry basis, daf: dried ash free basis, * calculated by
461 difference).

462

	PA [%db]		UA [%daf]					HHV [db]
	VM	A	C	H	N	S	O*	[MJ/kg]
Chlorella Vulgaris	76.26	13.11	59.06	8.81	11.39	0.66	20.08	21.57
Sewage Sludge	57.11	34.66	56.46	7.91	8.42	2.83	24.38	15.73

463

A detailed comparison of the results obtained from the basic characterization of Chlorella Vulgaris and sewage sludge was carried out in a previous work (Soria-Verdugo et al., 2017b), where these results were found to be similar to those reported in the literature by several authors.

4. Results and Discussion

4.1. TGA measurements

The capability of the TGA to reproduce inverse exponential temperature increases as a combination of a series of 25 linear temperature increases was checked. Figure 3 shows the time evolution of temperature measured by the TGA for the two final reactor temperatures of T_∞ = 550 ºC and T_∞ = 650 ºC and the two inverse exponential temperature profiles, with heating parameters c = 0.06 min^{-1} and c = 0.18 min^{-1}, tested. Despite the fact that the curves are composed of 25 constant heating rates, the inverse exponential form of the temperature profiles measured by the TGA is smooth. The measured temperature increases are depicted in Figure 3, and the fitting of these data to inverse exponential increases in the form of Eq. (2) resulted in determination coefficients $R^2 > 0.999$ in all cases. Therefore, the series of linear heating steps programmed to the TGA accurately describes the inverse exponential temperature increases required to validate the proposed LCM-DAEM model.

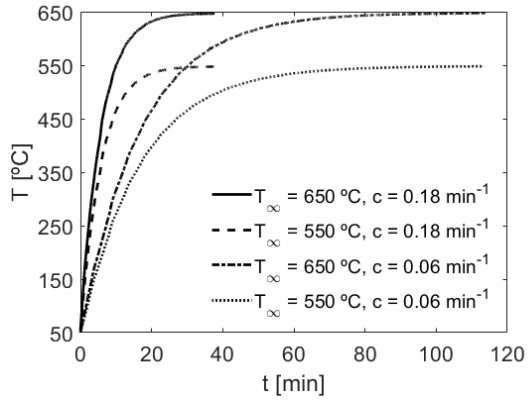

483

484 Figure 3. Temperature profiles measured in the TGA for different reactor
485 temperatures and heating parameters.

486 The TGA inverse exponential temperature profiles shown in Figure 3 were
487 employed to conduct pyrolysis tests using Chlorella Vulgaris and sewage sludge
488 samples. The TG curves obtained, depicting the time evolution of the pyrolysis
489 conversion α, are represented in Figure 4 for both samples. Clear differences are
490 observed for the pyrolysis tests conducted for different inverse exponential
491 heating parameters. A faster pyrolysis process occurs for the tests at c = 0.18
492 min^{-1} which last around 10 min, in contrast to the approximately 50 min required
493 by the pyrolysis experiments at c = 0.06 min^{-1}. There are also differences between
494 the TG curves corresponding to the same heating parameter and different reactor
495 temperatures due to the faster heating process required to attain a higher
496 temperature following the same inverse exponential temperature curve. Similar
497 TG curves were obtained for Chlorella Vulgaris and sewage sludge,
498 characterized in both cases by steep increases of the pyrolysis conversion with
499 time, as a consequence of the vigorous release of volatile matter, especially for
500 the faster heating, c = 0.18 min^{-1}. However, Figure 4 shows also differences for
501 the TG curves of Chlorella Vulgaris and sewage sludge for the lower heating
502 parameter of c = 0.06 min^{-1} tested. In these cases, the solid residue generated

503 after the release of highly volatile matter contained in sewage sludge, during
504 around 20 min, seems to react as time progresses, resulting in a slight increase
505 of the conversion with time during the final part of the pyrolysis test, t > 20 min.
506 In contrast, this effect was less pronounced for the Chlorella Vulgaris sample.

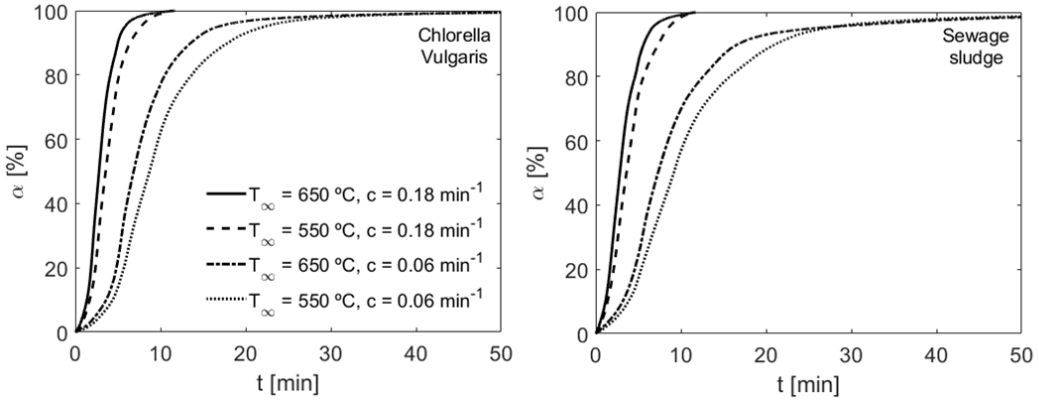

507

508 Figure 4. Pyrolysis conversion curves for Chlorella Vulgaris and sewage sludge.

509 **4.2. Validation of the LCM-DAEM model proposed**

510 The validation of the proposed LCM-DAEM model was based on the comparison
511 of the pyrolysis conversion measured in TGA with the predictions of the model
512 for both Chlorella Vulgaris and sewage sludge pyrolysis. This comparison was
513 carried out for reactor temperatures of T_∞ = 550 ºC and T_∞ = 650 ºC and for the
514 two inverse exponential temperature profiles tested, corresponding to heating
515 parameters of c = 0.06 min^{-1} and c = 0.18 min^{-1}. The prediction of the LCM-DAEM
516 model is obtained by solving the corresponding Arrhenius equation, i.e., Eq. (24)
517 for T_∞ = 550 ºC and Eq. (25) for T_∞ = 650 ºC, to determine the temperature of the
518 sample T for specific values of the pyrolysis conversion α. To that end, the
519 evolution of the pre-exponential factor A and the activation energy E of the
520 biomass sample with the pyrolysis conversion α should be known. The evolution
521 of A and E of Chlorella Vulgaris and sewage sludge with the pyrolysis conversion

522 α, for a range between 5% and 95% with intervals of 1%, was reported in Soria-
523 Verdugo et al. (2017b), and they can also be observed in the supplementary
524 material of this paper. These evolutions of the pre-exponential factor *A* and
525 activation energy *E* with the pyrolysis conversion α were obtained by applying the
526 simplified DAEM to TGA pyrolysis measurements conducted using nine different
527 constant heating rates.

528 The kinetic parameters of the pyrolysis reactions *A* and *E* reported in Soria-
529 Verdugo et al. (2017b) were introduced in the transcendental Arrhenius
530 equations, Eq. (24) for T_∞ = 550 ºC and Eq. (25) for T_∞ = 650 ºC. These Arrhenius
531 equations have no analytical solution; thus, they should be solved using some
532 simple numerical method such as the Newton-Raphson technique. The Arrhenius
533 equations were numerically solved for values of the pyrolysis conversion α
534 between 5% and 95% varying with intervals of 1%. The estimation of the
535 temperature *T* in the whole range of pyrolysis conversion α was determined, for
536 both Chlorella Vulgaris and sewage sludge, for pyrolysis reactor temperatures of
537 T_∞ = 550 ºC and T_∞ = 650 ºC, using the two inverse exponential temperature
538 profiles measured experimentally in TGA (heating parameters of c = 0.06 min^{-1}
539 and c = 0.18 min^{-1}) in the Arrhenius equations. Therefore, the complex combined
540 heat transfer and chemical kinetics problem of biomass pyrolysis is simplified with
541 the proposed LCM-DAEM model to solve a simple Arrhenius equation.

542 The predictions obtained from the proposed LCM-DAEM model for the evolution
543 of pyrolysis conversion α with temperature *T* were compared with the
544 experimental measurements performed in TGA. As an example, Figure 5
545 represents the α - *T* curves measured in TGA together with the LDM-DAEM

model estimations for the pyrolysis of both Chlorella Vulgaris and sewage sludge for the case of the lower reactor temperature and heating parameter, T_∞ = 550 ºC and c = 0.06 min^{-1}. The experimental curves of α versus T are obtained directly from the pyrolysis conversion curves shown in Figure 4, considering the temperature profile imposed by the TGA to convert time into temperature. The numerical results obtained from the LCM-DAEM model for the evolution of the pyrolysis conversion α with temperature T, obtained solving the corresponding Arrhenius equation and depicted in Figure 5 for a pyrolysis conversion range between 5% and 95% in intervals of 1%, are in good agreement with the experimental measurements carried out in TGA for both Chlorella Vulgaris and sewage sludge, even though these two biomass samples have a totally different composition compared to lignocellulosic biomass.

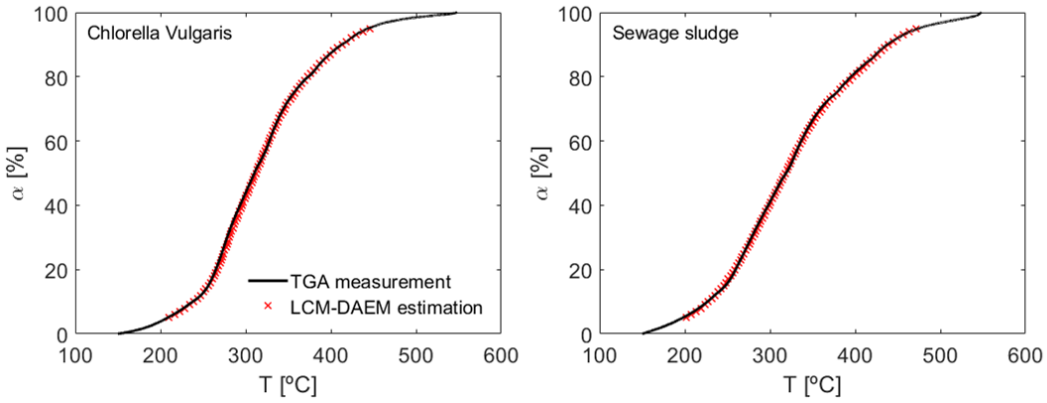

Figure 5. Comparison of the pyrolysis conversion of Chlorella Vulgaris and sewage sludge as a function of temperature experimentally measured in TGA and estimated by LCM-DAEM model for T_∞ = 550 ºC and c = 0.06 min^{-1}.

The results of the comparison between LCM-DAEM model predictions and TGA measurements for the rest of cases, i.e., different reactor temperatures and heating parameters, are similar to those shown in Figure 5. The Root Mean

565 Square Error (RMSE) was calculated for each case to quantify the deviation
566 between the LCM-DAEM estimations and the TGA experimental measurements
567 of temperature for each value of the pyrolysis conversion. These deviations of the
568 proposed LCM-DAEM model from the experimental measurements, regarding
569 the RMSE of temperature, are reported in Table 3 for the pyrolysis of both
570 Chlorella Vulgaris and sewage sludge under the different reactor temperatures
571 and heating parameters analyzed. The values obtained for the RMSE of
572 temperature are lower than 5 ºC in all cases, therefore, the proposed LCM-DAEM
573 model was proven to accurately describe the pyrolysis of biomass under inverse
574 exponential temperature increases, as those to which thermally small particles
575 are subjected.

576 Table 3. Root Mean Square Error (RMSE) [ºC] between temperature measured
577 by TGA and estimated by the LCM-DAEM model for each value of the
578 conversion between 5% and 95%.

	c = 0.06 min^{-1}		c = 0.18 min^{-1}	
	T_∞ = 550 ºC	T_∞ = 650 ºC	T_∞ = 550 ºC	T_∞ = 650 ºC
Chlorella Vulgaris	1.6	2.6	2.9	4.2
Sewage Sludge	1.5	3.8	2.3	4.7

579

580 The estimations of the proposed LCM-DAEM and the experimental pyrolysis
581 measurements conducted in TGA were also compared in terms of the average
582 relative error of temperature for each value of the pyrolysis conversion between
583 5% and 95%. This relative error was defined as the temperature deviation
584 between the model prediction and the experimental measurement divided by the

585 experimental temperature. The values of the average relative error obtained in
586 each case for both Chlorella Vulgaris and sewage sludge can be found in Table
587 4. An average relative error of temperature below 1% is obtained in all cases,
588 confirming the accuracy of the proposed LCM-DAEM model.

589 Table 4. Average relative error [%] between temperatures measured by TGA
590 and estimated by the LCM-DAEM model for each value of the conversion
591 between 5% and 95%.

	c = 0.06 min^{-1}		c = 0.18 min^{-1}	
	T_∞ = 550 ºC	T_∞ = 650 ºC	T_∞ = 550 ºC	T_∞ = 650 ºC
Chlorella Vulgaris	0.24	0.36	0.46	0.64
Sewage Sludge	0.23	0.42	0.30	0.71

592

593 **5. Conclusions**

594 A simple model combining the LCM and the simplified DAEM was proposed to
595 describe the pyrolysis process of thermally small biomass particles. The model is
596 based on an Arrhenius equation accounting for both the inverse exponential
597 temperature increase predicted by the LCM and the chemical kinetics described
598 by the simplified DAEM. The Arrhenius equation on which the model is based
599 was derived, for a variable reactor temperature, considering the pyrolysis
600 chemical kinetics data of several lignocellulosic biomass samples. Solving this
601 simple Arrhenius equation, the evolution of the pyrolysis conversion of thermally
602 small biomass particles subjected to a higher reactor temperature can be directly
603 estimated.

The validation of the model was based on TGA measurements of the pyrolysis of Chlorella Vulgaris and sewage sludge under inverse exponential temperature profiles. The deviation between the LCM-DAEM model predictions and the TGA measurements for the relation between pyrolysis conversion and temperature, regarding the RMSE of temperature, is lower than 5 ºC for all the cases tested. Concerning the average relative error between the temperatures estimated by the model and measured by the TGA, deviations below 1 % were obtained in all cases. Therefore, the proposed LCM-DAEM model was proven to accurately describe the evolution of the pyrolysis conversion with temperature for thermally small biomass particles. Furthermore, the difference in composition between the lignocellulosic samples, used to derive the Arrhenius equations, and the microalgae and sewage sludge, employed for the experimental measurements, guarantees the validity of the simple LCM-DAEM model proposed for a broad range of solid fuels, provided that the particle size is sufficiently small. Once the model was validated with TGA experimental measurements, it could be extended to consider also the dynamics of industrial pyrolysis reactors.

Acknowledgments

The authors express their gratitude to the BIOLAB experimental facility and to the “Programa de movilidad de investigadores en centros de investigación extranjeros (Modalidad A)” from the Carlos III University of Madrid (Spain) for the financial support conceded to Antonio Soria-Verdugo for a research stay at the German Aerospace Center DLR (Stuttgart, Germany) during the summer of 2018. Funding by Deutsches Zentrum für Luft- und Raumfahrt e. V. (DLR), the German Aerospace Center, is also gratefully acknowledged.

References

Anca-Couce A. Reaction mechanisms and multi-scale modelling of lignocellulosic biomass pyrolysis. Prog. Energ. Combust. 2016; 53, 41-79.

Bach Q.V., Chen W.H. Pyrolysis characteristics and kinetics of microalgae via thermogravimetric analysis (TGA): A state-of-the-art review. Bioresource Technol. 2017; 246, 88-100.

Basu P. Biomass gasification and pyrolysis - Practical design and theory. Elsevier Inc.; 2010.

Bleinstein N., Handelsman R.A. Asymptotic expansions of integrals, Dover Publications Inc, New York, 1987.

Cai J., Liu R. New distributed activation energy model: numerical solution and application to pyrolysis kinetics of some types of biomass. Bioresource Technol. 2008; 99, 2795-2799.

Cai J., Wu W., Liu R. An overview of distributed activation energy model and its application in the pyrolysis of lignocellulosic biomass. Renew. Sust. Energ. Rev. 2014; 36, 236-246.

Ceylan S., Kazan D. Pyrolysis kinetics and thermal characteristics of microalgae Nannochloropsis oculata and Tetraselmis sp. Bioresource Technol. 2015; 187, 1-5.

Coats A.W., Redfern J.P. Kinetic parameters from thermogravimetric data. Nature. 1964; 201, 68-69.

649 Czernik S., Bridgwater A.V. Overview of applications of biomass fast pyrolysis
650 Oil. Energ. Fuel. 2004; 18, 590-598.

651 Figueira C.A., Moreira P.F., Giudici R. Thermogravimetric analysis of the
652 gasification of microalgae Chlorella Vulgaris. Bioresource Technol. 2015; 198,
653 717-724.

654 Günes M., Günes S.K. Distributed activation energy model parameters of some
655 Turkish coals. Energy Sources Part A 2008; 30, 1460-1472.

656 Incropera F.P., De Witt D.P., Bergman T.L., Lavine A.S. Fundamentals of heat
657 and mass transfer, 6th ed., John Wiley & Sons, United States of America, 2007.

658 Li Z., Zhao W., Meng B., Liu C., Zhu Q., Zhao G. Kinetic study of corn straw
659 pyrolysis: comparison of two different three-pseudo component models.
660 Bioresource Technol. 2008; 99, 7616-7622.

661 Lin T., Goos E., Riedel U. A sectional approach for biomass: Modelling the
662 pyrolysis of cellulose. Fuel Process. Technol. 2013; 115, 246-253.

663 McKendry P. Energy production from biomass (part 2): conversion technologies.
664 Bioresource Technol. 2002; 83, 47-54.

665 Miura K. A new and simple method to estimate f(E) and $k_0(E)$ in the distributed
666 activation energy model from three sets of experimental data. Energ. Fuel. 1995;
667 9, 302-307.

668 Miura K., Maki T. A simple method for estimating f(E) and $k_0(E)$ in the distributed
669 activation energy model. Energ. Fuel. 1998; 12, 864-869.

670 Pattara C., Cappelletti G.M., Cichelli A. Recovery and use of olive stones:
671 Commodity, environmental and economic assessment. Renew. Sust. Energ.
672 Rev. 2010; 14, 1484-1489.

673 Sharma A., Pareek V., Zhang D. Biomass pyrolysis - A review of modelling,
674 process parameters and catalytic studies. Renew. Sust. Energ. Rev. 2015; 50,
675 1081-1096.

676 Sonobe T., Worasuwannarak N. Kinetic analyses of biomass pyrolysis using the
677 distributed activation energy model. Fuel 2008; 87, 414-421.

678 Soria-Verdugo A., García-Hernando N., Garcia-Gutierrez L.M., Ruiz-Rivas U.
679 Analysis of biomass and sewage sludge devolatilization using the distributed
680 activation energy model. Energ. Convers. Manage. 2013; 65, 239-244.

681 Soria-Verdugo A., Garcia-Gutierrez L.M., Blanco-Cano L., Garcia-Hernando N.,
682 Ruiz-Rivas U. Evaluating the accuracy of the Distributed Activation Energy Model
683 for biomass devolatilization curves obtained at high heating rates. Energ.
684 Convers. Manage. 2014; 86 1045-1049.

685 Soria-Verdugo A., Goos E., García-Hernando N. Effect of the number of TGA
686 curves employed on the biomass pyrolysis kinetics results obtained using the
687 Distributed Activation Energy Model. Fuel Process. Technol. 2015; 134, 360-371.

688 Soria-Verdugo A., Goos E., Arrieta-Sanagustín J., García-Hernando N. Modeling
689 of the pyrolysis of biomass under parabolic and exponential temperature
690 increases using the Distributed Activation Energy Model. Energ. Convers.
691 Manage. 2016; 118, 223-230.

692 Soria-Verdugo A., Morato-Godino A., Garcia-Gutierrez L.M., García-Hernando N.
693 Pyrolysis of sewage sludge in a fixed and a bubbling fluidized bed – Estimation
694 and experimental validation of the pyrolysis time. Energ. Convers. Manage.
695 2017a; 144, 235-242.

696 Soria-Verdugo A., Goos E., Morato-Godino A., García-Hernando N., Riedel U.
697 Pyrolysis of biofuels of the future: Sewage sludge and microalgae -
698 Thermogravimetric analysis and modelling of the pyrolysis under different
699 temperature conditions. Energ. Convers. Manage. 2017b; 138, 261-272.

700 Soria-Verdugo A., Goos E., García-Hernando N., Riedel U. Analyzing the
701 pyrolysis kinetics of several microalgae species by various differential and
702 integral isoconversional kinetic methods and the Distributed Activation Energy
703 Model. Algal Res. 2018; 32, 11-29.

704 Vand V. A theory of the irreversible electrical resistance changes of metallic films
705 evaporated in vacuum. Proc. Phys. Soc. 1943; 55, 222-246.

706 Várghegyi G., Szabó P., Antal M.J. Kinetics of charcoal devolatilization. Energ.
707 Fuel 2002; 16, 724-731.

708 Vyazovkin S.V., Lesnicovich A.I. Practical application of isoconversional
709 methods. Thermochim. Acta. 1992; 203, 177-185.

710 Wang Q., Wang H., Sun B., Bai J., Guan X. Interactions between oil shale and
711 its semicoke during co-combustion. Fuel 2009; 88, 1520-1529.

712 Wanjun T., Cunxin W., Donghua C. Kinetic studies on the pyrolysis of chitin and
713 Chitosan. Polym. Degrad. Stab. 2005; 87, 389-394.

714 Yan J.H., Zhu H.M., Jiang X.G., Chi Y., Cen K.F. Analysis of volatile species
715 kinetics during typical medical waste materials pyrolysis using a distributed
716 activation energy model. J. Hazard. Mater. 2009; 162, 646-651.

717

718 **List of figures**

728 **List of tables**